


SusE facilitates starch uptake independent of starch binding in *B. thetaiotaomicron*

Matthew H. Foley, Eric C. Martens and
Nicole M. Koropatkin *

Department of Microbiology and Immunology,
University of Michigan Medical School, Ann Arbor, MI
48109, USA.

Summary

The *Bacteroides thetaiotaomicron* starch utilization system (Sus) is a model system for nutrient acquisition by gut Bacteroidetes, a dominant phylum of gut bacteria. The Sus includes SusCDEFG, which assemble on the cell surface to capture, degrade and import starch. While SusD is an essential starch-binding protein, the precise role(s) of the partially homologous starch-binding proteins SusE and SusF has remained elusive. We previously reported that a non-binding version of SusD (SusD*) supports growth on starch when other members of the multi-protein complex are present. Here we demonstrate that SusE supports SusD* growth on maltooligosaccharides, and determine the domains of SusE essential for this function. Furthermore, we demonstrate that SusE does not need to bind starch to support growth in the presence of SusD*, suggesting that the assembly of SusCDE is most important for maltooligosaccharide uptake in this context. However, starch binding by proteins SusDEF directs the uptake of maltooligosaccharides of specific lengths, suggesting that these proteins equip the cell to scavenge a range of starch fragments. These data demonstrate that the assembly of core Sus proteins SusCDE is secondary to their glycan binding roles, but glycan binding by Sus proteins may fine tune the selection of glycans from the environment.

Introduction

The human gut microbiota performs critical tasks that promote host health and development (Stappenbeck

et al., 2002; Flint *et al.*, 2008; Round and Mazmanian, 2009; Wardwell *et al.*, 2011) including the mutualistic break down of complex carbohydrates (fiber) from our diet, (Flint *et al.*, 2008; Flint *et al.*, 2017). Dietary fiber processing begins at the bacterial cell surface via the action of one or more glycoside hydrolases or polysaccharide lyases that liberate smaller oligosaccharides that are harvested by the same or neighboring bacterial species (Cockburn and Koropatkin, 2016). For example, organisms in the gut such as *Ruminococcus bromii* process resistant starch into small fragments that can then cross-feed other species (Ze *et al.*, 2012). However, other bacteria such as *Bacteroides thetaiotaomicron* may employ a more ‘selfish’ mechanism for the processing of specific glycans such as yeast cell wall α -mannan in which the bacterium breaks α -mannan into fragments that it can select for uptake, limiting cross-feeding (Cuskin *et al.*, 2015). Understanding the molecular mechanisms employed by gut microbes to utilize dietary carbohydrates can foster the development of dietary strategies to manipulate the microbiota and improve health.

The Gram-negative Bacteroidetes are abundant members of the intestinal ecosystem in part due to their ability to efficiently acquire carbohydrates (Martens *et al.*, 2009; Ding and Schloss, 2014). The Bacteroidetes employ complexes of proteins, termed Sus-like systems, that localize to the cell surface and act in concert to bind, degrade and import glycans. Sus-like systems are encoded in polysaccharide utilization loci (PUL), gene clusters that are transcriptionally activated in response to a distinct carbohydrate substrate (Martens *et al.*, 2009). Some Bacteroidetes dedicate ~20% of their genomes to encoding PUL (Martens *et al.*, 2011). All PUL have at least one pair of proteins that share homology to SusC, a putative TonB-dependent transporter and SusD, a starch-binding protein, from the Starch utilization system (Sus) of *Bacteroides thetaiotaomicron* (Martens *et al.*, 2009; Terrapon *et al.*, 2015). Detailed biochemical studies of the glycolytic machinery and glycan-binding proteins from PUL that target pectin, β -glucan, xyloglucan, chitin and xylan, among others, have helped elucidate a general model of these systems by which carbohydrates are initially degraded at the cell

Accepted 7 March, 2018. *For correspondence. E-mail nkoropat@umich.edu; Tel. (+1) 734 647 5718; Fax (+1) 734 764 3562.

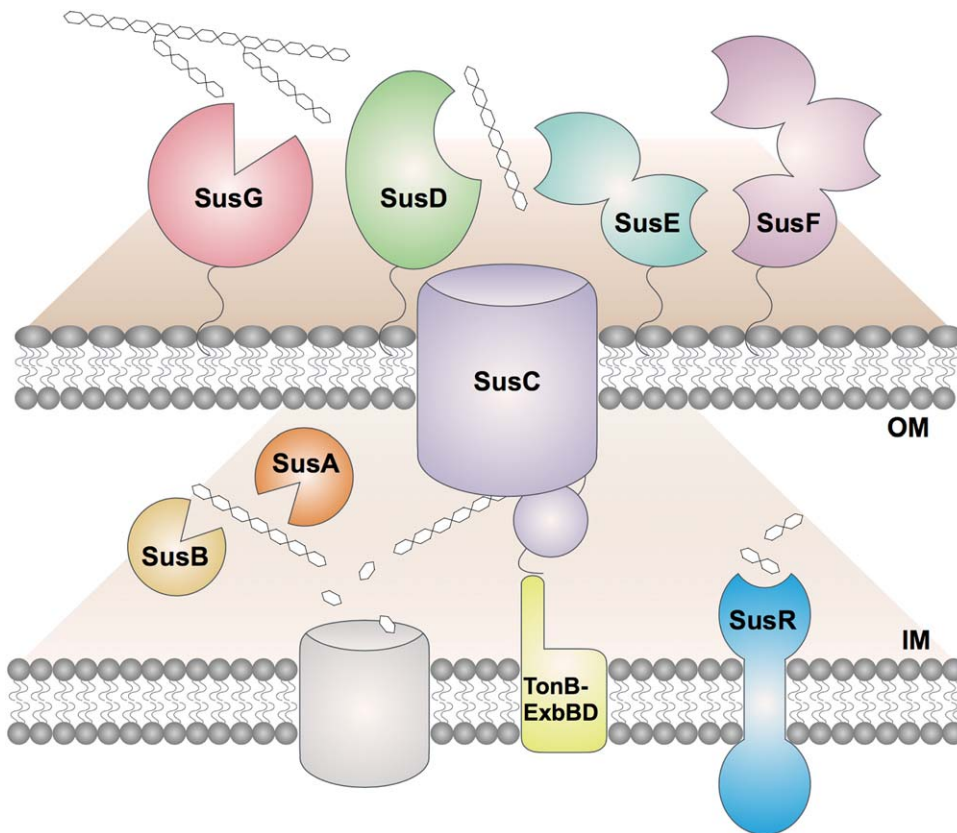


Fig. 1. Overview of the starch utilization system (Sus) in *B. thetaiotaomicron*. Starch is bound by the starch-binding lipoproteins SusDEF and the α -amylase SusG cleaves the polysaccharide to generate maltooligosaccharides that can be internalized by the TonB-dependent transporter SusC. The neopullulanase and α -glucosidase SusA and SusB, respectively, process the maltooligosaccharides to glucose that is introduced to the cytoplasm through an unknown transporter. The inner membrane-spanning protein SusR senses the disaccharide maltose and subsequently drives transcription of the *sus* locus.

surface and oligosaccharides are selected and imported into the cell via a SusCD-like complex (Larsbrink *et al.*, 2014, 2016; Rogowski *et al.*, 2015; Ndeh *et al.*, 2017; Tamura *et al.*, 2017).

The *B. thetaiotaomicron* Sus is an eight-gene locus that encodes five outermembrane proteins, SusCDEFG, involved in starch uptake (Tancula *et al.*, 1992) (Fig. 1). X-ray crystallographic structures of SusDEFG revealed eight distinct starch-binding sites among the four proteins (Koropatkin *et al.*, 2008; Koropatkin and Smith, 2010; Cameron *et al.*, 2012). SusG is the sole extracellular Sus enzyme and is required to process starch into maltooligosaccharides that are imported via the putative TonB-dependent transporter (TBDT) SusC (Reeves *et al.*, 1996; Shipman *et al.*, 1999). In the periplasm, maltooligosaccharides are depolymerized by SusA, a neopullulanase and SusB, an α -glucosidase (Smith and Salyers, 1991; D'Elia and Salyers, 1996a; Gloster *et al.*, 2008). The disaccharide maltose is recognized by the regulatory protein SusR, and activates *sus* transcription (D'Elia and Salyers, 1996b).

One important role of SusD during glycan transport is the capture of maltooligosaccharides for efficient import via SusC, which leads to increased levels of these sugars in the periplasm and triggers transcriptional activation of *sus* via SusR (Cameron *et al.*, 2014). We have

demonstrated that cells with a starch-binding-deficient allele of SusD, termed SusD*, are much less sensitive to the presence of maltooligosaccharides in the environment, requiring 100–1000x more sugar to achieve maximum transcription of the *sus* operon. SusD* expressing cells also lag longer than SusD-expressing cells when cultured on starch or maltooligosaccharides but not on glucose. However, the addition of small amounts of maltose, which upregulates *sus* but does not require Sus for uptake, partially relieves the lag seen with SusD* cells. These data suggested to us that the single starch-binding site of SusD is not required during steady-state growth of *B. thetaiotaomicron* on starch and maltooligosaccharides (i.e., when the *sus* operon is already upregulated) implying that SusE and SusF may provide substrate binding during transport (Cameron *et al.*, 2014). Seminal work performed by Salyers and colleagues demonstrated that SusC and SusD interact and that SusEF may modulate the SusCD interaction (Cho and Salyers, 2001). The recent structures of two SusCD-like complexes from *B. thetaiotaomicron* revealed that the SusD-like protein sits on top of the SusC-like transporter, with the putative substrate-binding site facing the channel (Glenwright *et al.*, 2017). In one of these complexes, multidomain PUL-encoded proteins resembling SusE and SusF co-purified with the

Table 1. Mutant Sus alleles used in this study

Mutant allele	Mutations (by protein residue number)	Effect	Reference
SusD*	W98A/N101A/W320A	No starch binding	(Cameron et al., 2014)
SusEb*	W192/K221A/Y229A/N252A	No starch binding at the Eb domain	(Cameron et al., 2012)
SusEc*	R326A/W336A/R350A	No starch binding at the Ec domain	(Cameron et al., 2012)
SusE*	W192/K221A/Y229A/N252A/ R326A/W336A/R250A	No starch binding at the Eb or Ec domains	(Cameron et al., 2012)
SusF*	W177A/K208A/W222A/D231A/W287A/ K323A/N356A/W396A/W442A/R456A	No starch binding at the Fa, Fb or Fc domains	(Cameron et al., 2012)
SusG ^{D498N}	D498N	Catalytically inactive (nucleophile mutant) SusG	(Koropatkin and Smith, 2010)
SusE ^{C21A}	C21A	Periplasmically localized SusE	(Cameron et al., 2012)
SusF ^{C20A}	C20A	Periplasmically localized SusF	(Cameron et al., 2012)

transporter, suggesting that other PUL-encoded proteins may interact with the SusCD-like complex. Co-immunoprecipitation of Sus-like proteins that target host sugars such as heparin, heparin sulfate and other *N*-linked glycoproteins also demonstrate that the cell-surface glycan-binding proteins physically interact (Renzi *et al.*, 2011; Cartmell *et al.*, 2017).

In this study, we investigated how the SusDEF lipoproteins and their starch-binding sites contribute to starch and maltooligosaccharide utilization by *B. thetaiotaomicron*. Using targeted mutations in SusDEF, we demonstrate that only SusE can compensate for the loss of starch binding by SusD (SusD*) during growth on maltoheptaose. Most strikingly, we observed that the starch-binding function of SusE is not required to support growth of the SusD* mutant on maltoheptaose. Finally, we reveal how the SusDEF starch-binding lipoproteins drive the preference of the Sus complex for maltooligosaccharides of different size ranges. Together, these results show that SusD and SusE do not require starch-binding sites to direct maltooligosaccharides through SusC, yet SusDEF have a profound impact on the selection of maltooligosaccharides. These insights enhance our understanding of polysaccharide substrate capture by *B. thetaiotaomicron* and, more broadly, carbohydrate utilization in the Bacteroidetes.

Results

SusE compensates for the loss of the *SusD* starch-binding site during growth on maltoheptaose

Enzymatic cleavage by the SusG enzyme liberates starch-derived maltooligosaccharides that are the primary substrates of the remaining four Sus outer-membrane proteins. To address the roles of SusE and SusF during growth on maltoheptaose, a model maltooligosaccharide, we created a series of genetic deletions and point mutants in the genes encoding these proteins and recombined these back into the *sus* operon via allelic

exchange in a Δtdk strain of *B. thetaiotaomicron*, referred to throughout as the wild-type strain. Alleles of *susDEFG* that have been mutated to abolish starch binding are labeled as Sus* mutants, and all have been previously characterized (Table 1). All strains used in this study or created within our previous studies are listed in Supporting Information Table S1. To determine how the SusEF proteins in our strains affect growth on starch or maltooligosaccharides, cell growth was monitored anaerobically in a 96-well plate reader. For each growth experiment, all strains were back-diluted 1:200 from minimal media with glucose or maltose, as noted, into both the test substrate (starch or maltooligosaccharide) as well as a glucose control. All of the 34 mutants reported in this study grew as the parent strain on glucose (Supporting Information Fig. S1), and achieve exponential phase at nearly the same time, verifying that all strains in each set of growth experiments were started at the same O.D. Therefore despite the limitations of the plate reader in resolving growth at low O.D., we feel confident that the dramatic differences in lag that we see with some of our phenotypes reflects biological differences among the strains and is not an artifact of our experimental set-up. When necessary, we performed a second growth experiment in culture tubes in order to better resolve strain difference.

As previously observed, *B. thetaiotaomicron* cells expressing SusD* grow on 2.5 mg ml^{-1} (2.17 mM) maltoheptaose despite an extended lag compared to the wild-type parent strain (Fig. 2A). This lag is associated with reduced transcriptional activation of the *sus* operon, presumably due to inefficient maltooligosaccharide uptake and reduced glycan levels in the periplasm (Cameron *et al.*, 2014). Growth on maltoheptaose is not dependent on extracellular processing by the surface enzyme SusG as SusD* Δ G cells grow the same as the SusD* strain. Additionally, cells lacking SusDEFG cannot grow on maltoheptaose, demonstrating that SusC alone is not sufficient to support growth on maltoheptaose. In order to better resolve the apparent lag

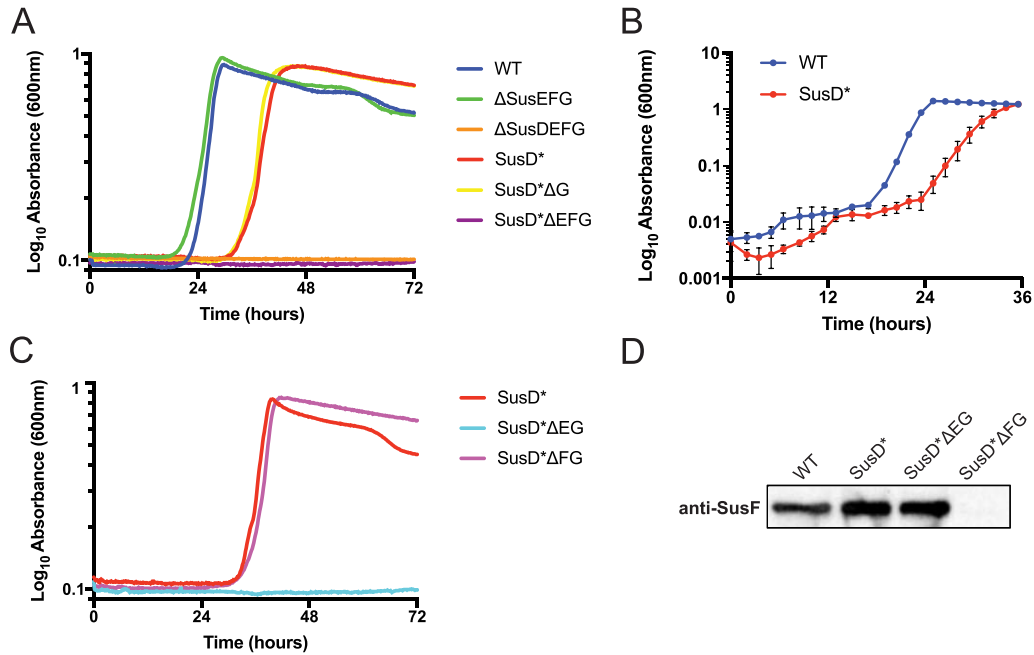


Fig. 2. SusE compensates for the loss of the SusD starch binding site during growth on maltoheptaose.

A and C. Average growth curves of *B. thetaiotaomicron* strains expressing SusD* in different *sus* mutant backgrounds cultured on 2.5 mg ml⁻¹ maltoheptaose. Identical growth experiments in glucose are shown in Supporting Information Fig. S1A and B.

B. Average growth curves of wild-type (WT) and SusD* *B. thetaiotaomicron* cultured on 2.5 mg ml⁻¹ maltoheptaose with absorbance measured manually in a spectrophotometer. Biological triplicate cultures were cultured in glucose then back-diluted 1:800 into minimal media with maltoheptaose.

D. Western blot using anti-SusF serum against whole cell lysates from WT, SusD*, SusD*ΔEG and SusD*ΔFG cultures. Strains were cultured in minimal media containing 5 mg ml⁻¹ maltose and were arrested in logarithmic phase then normalized by O.D.₆₀₀ for loading in SDS-PAGE.

between the wild type and SusD* strain, a second growth experiment with biological triplicate cultures on 2.5 mg ml⁻¹ maltoheptaose was performed in culture tubes and the O.D.₆₀₀ was assessed in a spectrophotometer to resolve lower O.D.₆₀₀ readings (Fig. 2B). The growth of these strains revealed a biphasic curve with an early exponential expansion containing similar specific growth rates at O.D.₆₀₀ = 0.01 between wild-type (0.26 ± 0.13 h⁻¹) and SusD* (0.27 ± 0.05 h⁻¹). A larger, second exponential phase revealed an increased growth rate at O.D.₆₀₀ = 0.2 for wild-type (0.68 ± 0.07 h⁻¹) compared to SusD* (0.40 ± 0.09 h⁻¹). SusD* displays an initial lag before growth as well as a slower second exponential growth rate relative to wild-type, and both contribute to the apparent lag observed in the plate reader. The precise difference between growth rates in the culture tubes versus the plate reader is unclear, but not entirely unexpected when growth conditions change. We suspect that evaporation in the plate reader set-up may contribute to these effects. The growth defects seen in SusD* are likely representative of the apparent lag phenotypes observed in other strains in this study.

The ability to grow on maltoheptaose is abolished when the SusD* allele is combined with loss of SusEFG, hinting at a compensatory role for SusE and/or SusF. Upon

further analysis, individual deletions of *susEG* and *susFG* revealed that the loss of SusE, but not SusF, prevented the growth of cells expressing SusD* (Fig. 2C). This phenotype is not the result of a polar mutation from the *susE* deletion as immunoblots of whole cells with anti-SusF antibodies demonstrate the expression of *susF* (Fig. 2D). These data suggest a unique role for SusE during growth on maltooligosaccharides.

SusE and SusF share multiple structurally homologous but functionally divergent domains

That SusE and SusF display divergent functions within Sus is noteworthy as SusE and SusF contain conserved structural characteristics suggesting redundant roles during starch catabolism. Both proteins have multimodular structures comprised of β -sheet rich starch-binding domains in tandem with an N-terminal Ig-like fold domain (Cameron *et al.*, 2012). Proline residues are present between sequential domains of both proteins that presumably limit conformational flexibility, with the exception that SusE contains a putative flexible linker between the N-terminal domain and its first starch-binding domain, the Eb domain (see Fig. 3B for schematic). SusF has three starch-binding domains, Fa, Fb

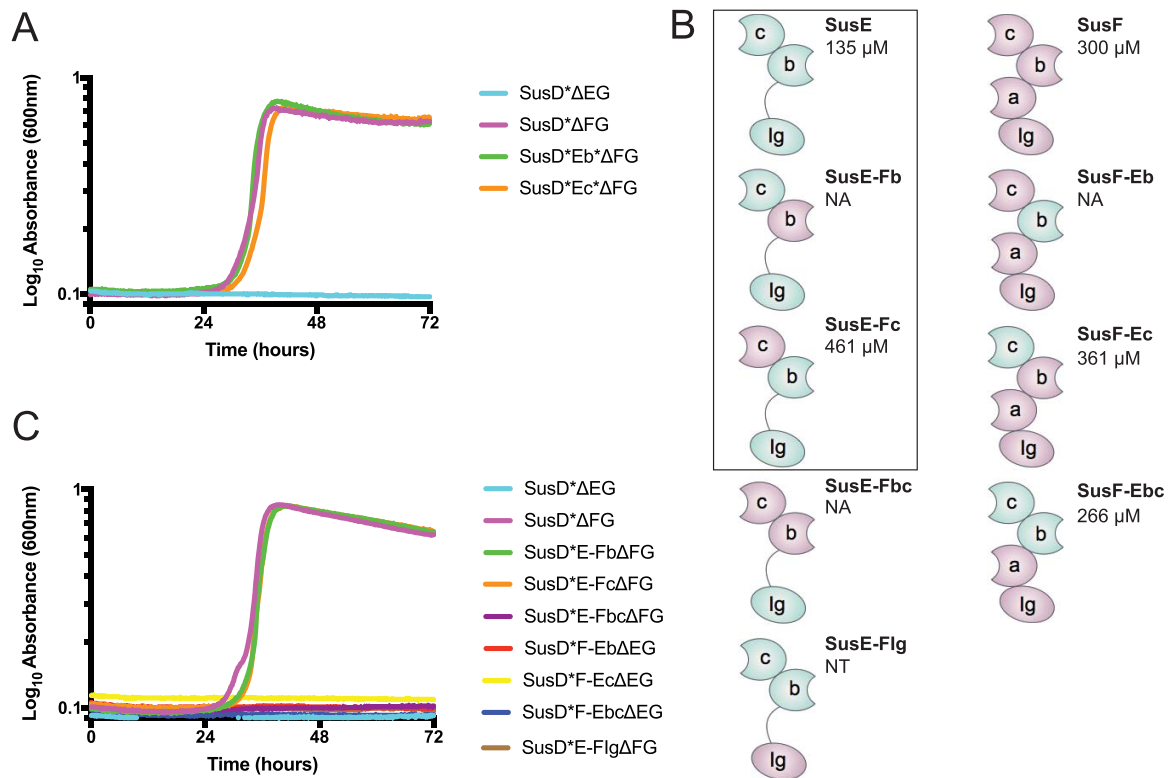


Fig. 3. SusE and SusF are composed of functionally unique, but structurally homologous starch-binding domains.

A. Average growth curves of *B. thetaiotaomicron* strains expressing single starch-binding site mutants of SusE on 2.5 mg ml⁻¹ maltoheptaose. Identical growth experiments in glucose are shown in Supporting Information Fig. S1C.

B. Schematic of chimeric SusE and SusF domain structures. The K_d (μM) of each chimera for maltoheptaose as measured by isothermal titration calorimetry (average of three replicates) is reported. The K_d (μM) of the recombinant wild-type proteins is displayed for reference, as previously reported (Cameron *et al.*, 2012). A box is placed around constructs that support growth in *B. thetaiotaomicron* expressing SusD*.

NA denotes chimeric constructs that did not express in *E. coli*. NT denotes chimeric constructs not tested for recombinant expression. C. Average growth curves of *B. thetaiotaomicron* strains expressing chimeric SusE and SusF on 2.5 mg ml⁻¹ maltoheptaose. The mutants that displayed growth were SusD*ΔFG (light purple), SusD*E-FbΔFG (green) and SusD*E-FcΔFG (orange). Identical growth experiments in glucose are shown in Supporting Information Fig. S1D.

and Fc and SusE has two, Eb and Ec, named for their homology to the domains of SusF (Fig. 3B). Among all five domains, Ec has the highest binding affinity for maltoheptaose and starch (Cameron *et al.*, 2012). The Ig-like fold of SusE (E_N) was predicted to be similar to that of SusF (F_N).

To identify the domains of SusE that promote growth on maltoheptaose in the SusD* strain, we utilized mutant alleles of *susE* that we have previously reported that contain only one viable starch-binding site (Cameron *et al.*, 2012). The SusEb* and SusEc* expressing strains, in which the Eb and Ec domain respectively cannot bind starch, were exchanged into the *B. thetaiotaomicron* chromosome in place of *susE*. Expression of these single-binding mutants with the SusD* allele revealed that both SusD*Eb* or SusD*Ec* strains grow on maltoheptaose with similar kinetics, demonstrating that both of the SusE starch-binding sites can compensate for the SusD* mutation (Fig. 3A). This was surprising as the K_d of Ec for maltoheptaose is ~20 μM and 50-fold higher than both

SusEb and SusD (Cameron *et al.*, 2012). Despite a K_d of 1 mM for maltoheptaose, native SusD efficiently supports growth on maltoheptaose emphasizing that high affinity binding to maltoheptaose is not required for transport through SusC (Fig. 2A).

Given that either starch-binding site of SusE is adequate for growth on maltoheptaose, we sought to determine which domains of SusE must be present for growth. Exploiting the structural homology of SusE and SusF, we created a set of chimeric proteins in which Eb and Ec or Fb and Fc were swapped individually or in combination between SusE and SusF (Fig. 3B). Immunofluorescent microscopy of fixed whole cells verified that these chimeric proteins were expressed by *B. thetaiotaomicron* and trafficked to the outer membrane (Supporting Information Fig. S2); we have demonstrated that cells expressing site-directed mutants of SusE and SusF (SusE^{C21A} and SusF^{C20A}) that retain the proteins in the periplasm cannot be labeled (Cameron *et al.*, 2012). Recombinant expression and purification of these

chimeras was performed to verify starch binding, however three of the seven mutants, SusE-Fb, SusE-Fbc and SusF-Eb, were not soluble when expressed in *E. coli*. Since all of these proteins expressed and correctly trafficked in *B. thetaiotaomicron* we speculate that there may be some aspects of protein folding that are unique to *B. thetaiotaomicron*. Proteins that could be expressed in *E. coli* were assayed for maltoheptaose binding by isothermal titration calorimetry, and displayed K_d values similar to the wild-type proteins (Fig. 3B, Supporting Information Fig. S3) (Cameron *et al.*, 2012).

When grown on maltoheptaose, chimeric SusE containing only one starch-binding SusF domain (SusD*E-Fb Δ FG and SusD*E-Fc Δ FG) was able to support growth as was the wild-type SusE allele in *B. thetaiotaomicron* expressing SusD* (Fig. 3C). If both domains Eb and Ec were replaced with Fbc (SusD*E-Fbc Δ FG), then *B. thetaiotaomicron* could not grow, indicating that at least one of the SusE starch-binding domains is required. While the SusE-Fbc mutant could not be isolated from *E. coli*, the SusE-Fb allele that supports growth also could not be obtained recombinantly, supporting that lack of soluble expression in *E. coli* does not necessarily mean a lack of functional or correctly folded protein in *B. thetaiotaomicron*. None of the SusF chimeras possessing Eb or Ec domains were able to rescue growth in the SusD* expressing mutant. These observations suggest that the SusE starch-binding domains are necessary, but also that its N-terminal domain may be important. Indeed, our SusE mutant allele expressing the SusF N-terminal Ig-like domain (SusD*E-Fig Δ FG), did not support growth on maltoheptaose although this chimera is expressed on the surface of the cell (Supporting Information Fig. S2). Taken together, the ability of SusE to compensate for SusD* is dependent on its distinctive domains at both the N and C-terminus. However, we cannot rule out that the putative flexibility of SusE is also a required facet of its function. Note that the chimeric SusE proteins were created to retain the putative linker between the N-terminal domain and the following Eb or Fb domain.

Maltoheptaose binding by SusE is not required to promote growth

We have recently reported that immunoprecipitation of SusD results in co-isolation of both SusE and SusC, so we hypothesized that SusE provides a starch-binding function within the proximity of SusC to guide glycans into the transporter (Tuson *et al.*, 2018). Previous work provided evidence for an interaction between SusE and SusF, so we reasoned that SusF might contribute to glycan import via an interaction with SusE proximal to the

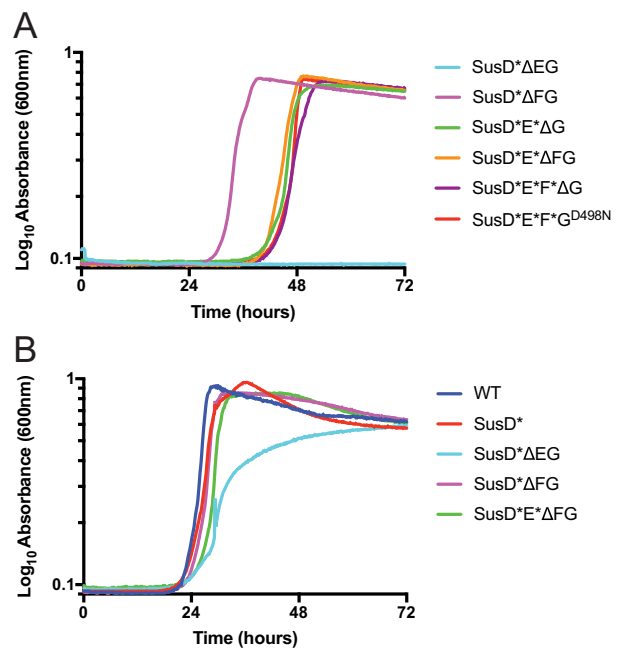


Fig. 4. SusE does not require starch-binding sites for its unique functionality.

(A) Average growth curves of *B. thetaiotaomicron* strains expressing starch-binding deficient SusD*E* in various *sus* mutant backgrounds on 2.5 mg ml⁻¹ maltoheptaose or (B) 2.5 mg ml⁻¹ maltoheptaose supplemented with 0.5 mg ml⁻¹ maltose. Identical growth experiments in glucose are shown in Supporting Information Fig. S1E and F, and on 0.5 mg/maltose alone in Supporting Information Fig. S5.

SusCD complex (Cho and Salyers, 2001). However, the SusD*E* Δ G (expressing wild-type SusF), SusD*E* Δ FG and SusD*E*F* Δ G strains grow on maltoheptaose with an extended lag phase compared to the SusD* Δ FG that expresses a wild-type SusE (Fig. 4A). We tested whether the additional lag from the SusD*E* strain could be rescued by a SusF chimera that has one or more domains of SusE. Interestingly, the only chimeric SusF that had any effect on growth of the SusD*E* strain was SusF-Ec, which abolished growth (SusD*E*F-Ec Δ G, Supporting Information Fig. S4). Yet, SusF-Ec does not prevent growth when co-expressed with wild-type SusE (SusD*F-Ec Δ G, Supporting Information Figs S1J and S4). We speculate that the Ec domain on SusF-Ec is interfering with the Ec domain on SusE*, preventing its function in maltoheptaose transport. We also tested if the starch-binding sites on SusG enhance growth on maltoheptaose in the presence of SusD*E*F* as our previous work suggests that SusG dynamically interacts with the Sus complex (Karunatilaka *et al.*, 2014). However, a catalytically dead allele of SusG (SusG^{D498N}) does not improve growth on maltoheptaose (Fig. 4A).

The major observable difference in growth between our mutant strains is in the apparent lag, which occurs

when these strains are cultured on maltoheptaose, not glucose (Supporting Information Fig. S1). We attribute this lag to a defect in starch 'sensing,' or rather how quickly *sus* transcription is activated to support growth on starch; we have demonstrated previously that SusD* expressing cells require 100–1000x more sugar to maximally induce *sus* compared to wild-type cells (Cameron *et al.*, 2014). However, the addition of 0.5 mg ml⁻¹ maltose, which does not require Sus for import and alone supports minimal growth of the strains (Supporting Information Fig. S5), can upregulate *sus* and alleviate this lag (Cameron *et al.*, 2014). To examine how sensing might be affecting our mutants, we cultured several SusD* mutant strains in minimal media with 5 mg ml⁻¹ maltose, then subcultured into 2.5 mg ml⁻¹ maltoheptaose with 0.5 mg ml⁻¹ maltose. By inducing the *sus* operon with maltose, all strains grew comparably to wild-type with the exception of SusD*ΔEG, which now displayed growth on maltoheptaose but had a kinetic defect and lower maximum culture density (Fig. 4B). Thus, it is likely that in the absence of maltose, a SusD*ΔEG strain cannot efficiently import and accumulate sugar to sufficient levels required to activate transcription and increase Sus protein levels on the cell surface; this type of kinetic coordination between the glycan levels for transcriptional activation and the activity of the periplasmic enzymes has been reported for the chondroitin sulfate and heparin targeting Sus-like systems in *B. thetaiotaomicron* (Raghavan *et al.*, 2014). However, the growth defect of the SusD*ΔEG strain on maltoheptaose plus maltose suggests that even when *sus* is activated, the presence of SusE with SusD* is required for effective maltoheptaose import. Taken together, these data support that SusE, but not SusF or SusG, displays unique functionality during growth on maltooligosaccharides, and that its ability to support glycan uptake is not entirely dependent on its ability to bind sugar.

Substrate binding by SusE provides a competitive advantage during growth on starch

Although maltoheptaose is a useful substrate to study the mechanism of maltooligosaccharide uptake, we wanted to know if SusE is similarly important for utilization of a starch polysaccharide like amylopectin. SusG is required for growth on starch, but in-frame deletions of *susEF* affect SusG transcription (Reeves *et al.*, 1997; Cameron *et al.*, 2014). Therefore we used the periplasmically localized mutants SusE^{C21A} and SusF^{C20A} (Cameron *et al.*, 2014) to test growth on starch in the absence of cell surface SusE and SusF. Cells were grown on maltose, then back-diluted into 5 mg ml⁻¹ maize amylopectin with 0.5 mg ml⁻¹ maltose to assess

growth phenotypes. As before, 0.5 mg ml⁻¹ maltose alone supports a low level of growth for all strains (Supporting Information Fig. S6). *B. thetaiotaomicron* expressing SusD grows on starch without SusE or SusF on the cell surface (Cameron *et al.*, 2014) (Fig. 5A, SusE^{C21A} and SusF^{C20A}). Cells expressing SusD* alone or in combination with SusE^{C21A}, SusF^{C20A} or SusE* grow on starch but display a biphasic growth pattern with a more severe defect in the first phase. To assess the differences in growth rates, we quantified specific growth rates for each strain on glucose and starch during early (O.D.₆₀₀ = 0.35) and late (O.D.₆₀₀ = 0.75) exponential growth (Supporting Information Fig. S7). Across the strains, growth on glucose was within standard error at both time points. On starch, cells expressing SusD were slightly faster in the first phase though not significantly so from the SusD* expressing strains (Supporting Information Fig. S7). However, during late exponential growth on starch there was a significant decrease in growth rates in strains that expressed SusD* compared to those that expressed wild-type SusD, though there was no statistically significant difference among the SusD* expressing strains (Fig. 5B).

In order to verify the apparent similarities in growth for the SusD* mutants, we cultured the SusD*E^{C21A}, SusD*F^{C20A} and SusD*E* strains in culture tubes on 5 mg ml⁻¹ amylopectin with 0.5 mg ml⁻¹ maltose, as described earlier (Supporting Information Fig. S8A). To capture growth at lower initial concentrations of cells, we back-diluted biological triplicate cultures 1:800 into starch instead of 1:200 as performed for the plate reader assays. The overall phenotypes among these three strains appeared similar in both modalities and there are no significant differences in the apparent growth rates in culture tubes. Most notably SusD*E^{C21A} displayed a reduced maximum culture density with respect to SusD*F^{C20A} and SusD*E* suggesting that, although its growth rate is comparable to that of SusD*-expressing strains, SusE is needed to access the same level of starch in the media. Together, these observations support the idea that starch-binding by SusD is important for starch import, especially as starch may become limited in later time points. That the presence of SusE was not a requirement for growth was surprising, but SusG may be compensating for this, either via its additional starch-binding sites or by generating small oligosaccharides such as maltose and glucose (Koropatkin and Smith, 2010).

Although the growth rates displayed among the SusD* variants were similar, we wanted to know if the competitive fitness of *B. thetaiotaomicron* expressing SusD* was influenced by the presence of SusE, SusF, or SusE*. We performed *in vitro* competition experiments by co-culturing the SusD*E^{C21A} strain with either SusD*F^{C20A}

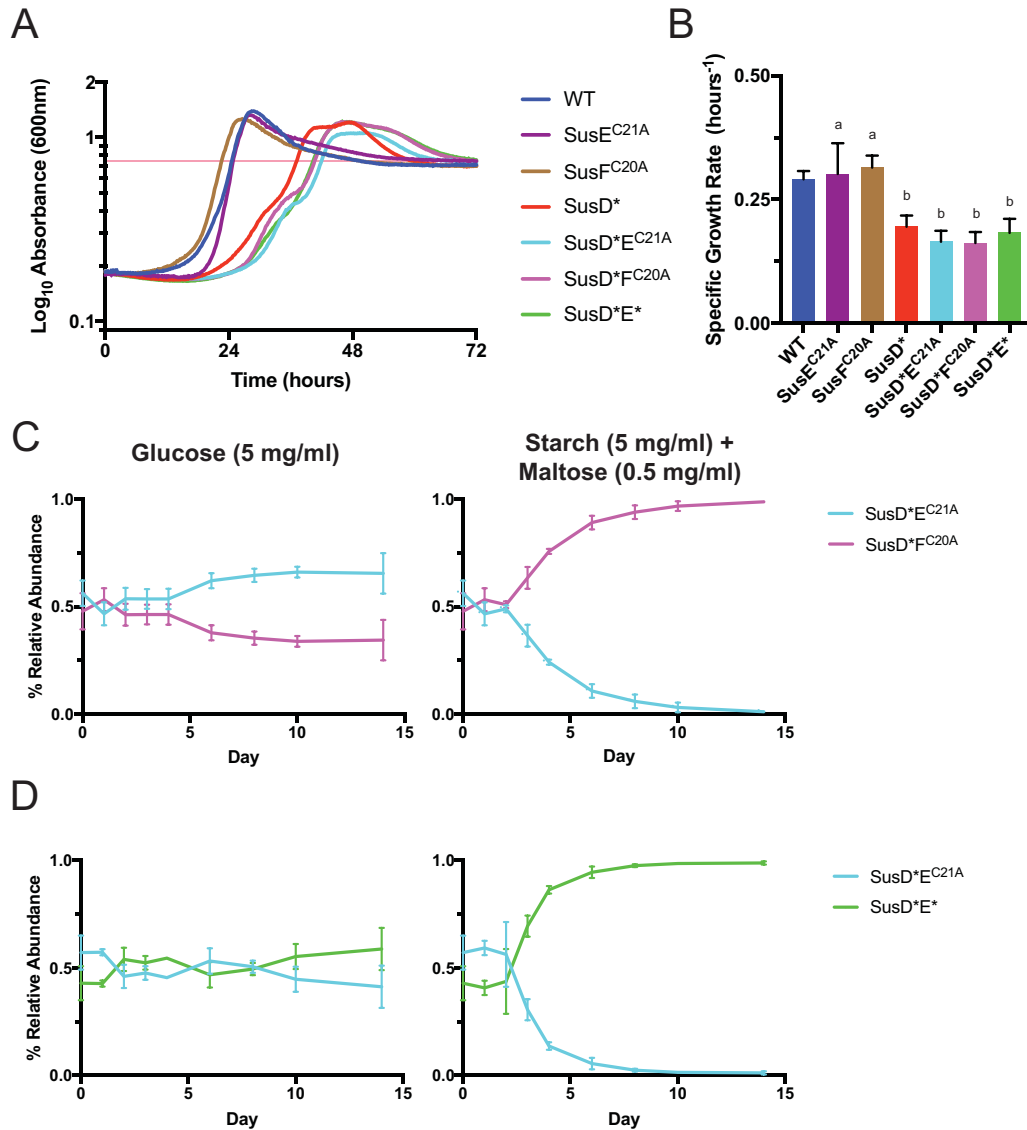


Fig. 5. SusE provides a competitive advantage during growth on starch

A. Average growth curves of *B. thetaiotaomicron* strains expressing periplasmically localized SusE (C21A) and SusF (C20A) in combination with SusD on 5 mg ml⁻¹ maize amylopectin supplemented with 0.5 mg ml⁻¹ maltose. Identical growth experiments in glucose are shown in Supporting Information Fig. S1G and for 0.5 mg maltose alone in Supporting Information Fig. S6. The horizontal pink line indicates an O.D.₆₀₀ of 0.75 at which specific growth rates, shown in panel B, were calculated for all strains.

B. Specific growth rates for all strains ($n = 3$) grown in panel (A). Bars denoted with the letter 'a' are not statistically significantly different from each other or WT. Bars denoted with the letter 'b' are not significantly different from each other but are different from WT with a P value < 0.05 . Statistically significant differences were determined using the two-tailed unpaired Student's t test.

C and D. *In vitro* competitions of barcoded SusD* mutants in 5 mg ml⁻¹ glucose or 5 mg ml⁻¹ maize amylopectin with 0.5 mg ml⁻¹ maltose. Relative abundance was calculated as the percent composition of a strain's DNA relative to the total DNA in the sample.

or SusD*E*. These mutants were genetically tagged and passaged each day into minimal media containing glucose or starch and the relative abundance of each strain was quantified by qPCR (Fig. 5C and D). The competitions in glucose may have displayed some stochastic changes in the abundance over time since it is unlikely the SusD*E^{C21A} mutant is better suited for growth on glucose than SusD*F^{C20A}; this seems likely given the

larger experimental error of the specific growth rates on glucose (Supporting Information Fig. S7). Nonetheless, growth on starch resulted in a drastic decrease in the abundance of SusD*E^{C21A}, as it was outcompeted by both SusD*F^{C20A} and SusD*E* within the same two week time frame. These results not only underscore that SusE does not need to bind starch to support growth, but also raise the possibility that SusE provides a fitness

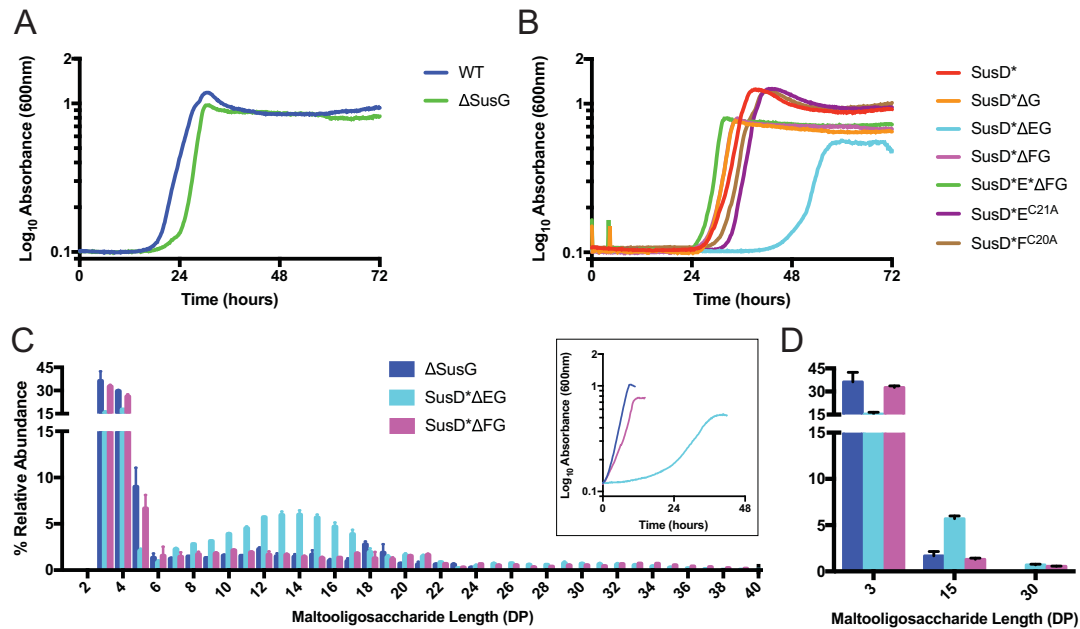


Fig. 6. Starch-Binding Proteins Facilitate the Uptake of Maltooligosaccharides in a Size Dependent Manner

A. Average growth curves of *B. theta* WT and Δ SusG strains on 5 mg ml^{-1} DP10–40 maltooligosaccharide mix. Identical growth experiments in glucose are shown in Supporting Information Fig. S1H.

B. Average growth curves of *B. theta* *SusD** expressing mutants on 5 mg ml^{-1} DP10–40. Identical growth experiments in glucose are shown in Supporting Information Fig. S1I.

C. Relative abundance of DP3–DP40 maltooligosaccharides in cell-free culture supernatants at stationary phase ($n = 2$). Maltooligosaccharides were purified from media components resulting in the loss of glucose and maltose.

D. Enlargement of representative small (DP3), medium (DP15) and large (DP30) maltooligosaccharides in cell-free culture supernatant of stationary phase cultures. Error bars indicate standard deviations across two biological replicates.

advantage by facilitating glycan uptake from the environment.

Surface starch-binding proteins coordinate oligosaccharide uptake based on their length

In the Bacteroidetes, oligosaccharides are generated from carbohydrate-active enzymes anchored to the cell surface or secreted via outer membrane vesicles into the environment (Elhenawy *et al.*, 2014; Rakoff-Nahoum *et al.*, 2014; Grondin *et al.*, 2017). Our data suggest that surface glycan-binding proteins like SusD, SusE and SusF are important for optimal glycan uptake through SusC, and we hypothesized that these starch-binding proteins could drive the preferential uptake of certain lengths of maltooligosaccharides. To test this we grew *B. theta* on a mixture of maltooligosaccharides spanning 1–40 glucose units (a commercial preparation marked as DP10–40, but HPAEC-PAD analysis of the starting mixture revealed the presence of smaller sugars ranging from DP1 to 10. DP = degree of polymerization of a chain of α 1,4-linked glucose residues) (Supporting Information Figs S9A and S10). All HPAEC-PAD chromatograms reported in this study are

compiled within Supporting Information Fig. S10. Glucose, maltose and maltotriose all support the growth of *B. theta* independent of Sus (Tancula *et al.*, 1992), but the majority of glycans in the mixture are $> \text{DP}7$ (Supporting Information Fig. S9A). Longer sugars in the range of DP32–40 fell below our detection limit here, but were detected in subsequent experiments. We considered that some of the longer oligosaccharides ($> \text{DP}7$) might not be transported efficiently, or at all, in the absence of SusG. Consistent with this notion, we observed that Δ SusG grows to a noticeably lower maximum O.D. compared to wild-type (Fig. 6A). Furthermore, we found this trend to be consistent across all other strains that lack SusG (Fig. 6B). Growth on DP10–40 by *SusD**, *SusD**E^{C21A} and *SusD**F^{C20A} all displayed similar kinetics, likely due to the enzymatic activity of SusG. Conversely, *SusD** Δ G, *SusD** Δ FG and *SusD**E Δ FG grew similarly on the DP10–40 mixture but the combination of starch-binding deficient mutations and loss of SusG resulted in these strains exhibiting an even lower maximum O.D. Consistent with a unique and important role in oligosaccharide uptake, the growth of *SusD** Δ EG had a notably longer lag and the lowest maximum O.D. among these strains, underscoring the

importance of SusE during starch uptake. The growth of SusD* Δ EG on DP10–40 is likely supported by the presence of maltose which induces *sus*.

To examine which maltooligosaccharides are depleted over time during growth, we grew Δ SusG on DP10–40 and measured glycan content in cell free supernatants from lag, exponential and stationary phase (Supporting Information Fig. S9B). Note that the preparation of media samples for HPAEC-PAD analysis resulted in the loss of glucose and maltose, and so these glycans are omitted from the analysis. Lag and exponential phase Δ SusG cultures had a similar distribution of oligosaccharides with a significant increase in the relative abundance of DP3 and DP4 in stationary phase (Supporting Information Fig. S9C). An increase in a sugar's relative abundance within the sample indicates that it is either being generated from the breakdown of a larger oligosaccharide, or it is being imported less frequently compared to other sugars, or both. Because we can detect glycolytic activity in Δ SusG culture supernatants due to the presence of intracellular or secreted enzymes within culture supernatants, we attribute the increase of DP3 and DP4 abundance at least partially to enzymatic activity (Supporting Information Fig. S11). Interestingly, there was a dramatic decrease in DP5–DP16 but an increase in DP17 content and steady levels of larger DP sugars from exponential to stationary phase (Supporting Information Fig. S9C and D). If unidentified glycolytic activity in the supernatant were wholly responsible for the loss of mid-range glycans we would expect a concomitant decrease in larger glycans as well, rather than a discrete increase in glycans of a particular DP length. Therefore we conclude from these data that the SusCDEF complex can import, and may select for, maltooligosaccharides of DP5–16.

We investigated the contributions of SusE and SusF to maltooligosaccharide preference by characterizing the portfolio of oligosaccharides in the media from parallel cultures of SusD* Δ FG, SusD* Δ EG and Δ SusG cells at stationary phase from growth on DP10–40. Once again, these strains displayed different growth kinetics and maximum culture densities, suggesting inefficient or selective uptake of certain glycans in the mixture (Fig. 6B and C inset). Like the first Δ SusG growth experiment, there is an enrichment of DP3–4 compared to other sugars, which may be because these are less frequently taken up, and there is likely some glycolytic activity in the media. Interestingly, sugars > DP23 were not found in Δ SusG cultures but were detected in SusD* Δ FG and SusD* Δ EG cultures, which may in part explain why these strains grow to a lower maximum O.D. SusD* Δ EG, which displays the most severe growth defect on DP10–40, is less efficient at taking up sugars DP7–18 and removes more of the small sugars 3–5

compared to Δ SusG and SusD* Δ FG cells. These data suggest that SusE is needed to efficiently access mid-range and longer sugars, and in the absence of SusE the cells may need to scavenge smaller sugars to support growth (Fig. 6D). Although the energetics of maltooligosaccharide import in the Bacteroides is largely unknown, the uptake of mid-length glycans through the Sus likely minimizes the number of transport events needed to support growth and may be a cost-effective strategy for glycan capture.

Discussion

Members of the gut microbiota compete for carbon and energy sources to survive in the densely populated colonic environment and the Bacteroidetes that dominate this niche rely on sets of cell surface proteins to recognize, degrade and import dietary polysaccharides. Glycan transport across the outer membrane is a critical feature of these systems that allows for the complete depolymerization of polysaccharides in the periplasm, which prevents the release of monosaccharides to neighboring species (Cuskin *et al.*, 2015). Hence, understanding how these bacteria import carbohydrates can provide knowledge for the strategic manipulation of select species in the gut. Here, we investigate glycan uptake via the prototypical Sus of *B. thetaiotaomicron*. Our findings have uncovered that the transporter SusC imports maltooligosaccharides in a manner that requires SusD and SusE, but is not contingent on their capacity for starch-binding, suggesting assembly of the complex is most important. Furthermore, these data suggest that the protein–protein interactions that dictate Sus complex assembly can tune how the cell acquires starch. These unexpected observations raise further questions about the underlying mechanisms of glycan transport by homologous Sus-like systems, particularly the relationship between SusC-like TBDTs and their cognate glycan-binding proteins. Two recent crystal structures of *B. thetaiotaomicron* SusCD-like complexes reveal that the SusD-like protein sits atop the SusC TonB-dependent transporter (TBDT), with the ligand-binding site directed into the opening of the barrel (Glenwright *et al.*, 2017). Molecular dynamics simulations of the complex for peptide import reveal that binding of the ligand by SusD protein and the internal plug of the TBDT stabilizes the closed complex, triggering the import event. In the absence of ligand, SusD can open to repeat this cycle. A difference between the two SusCD-like crystal structures was the presence of additional PUL-encoded lipoproteins that co-purified with the complex. The putative peptide-targeting SusCD-like complex included proteins BT2261–2264, with two

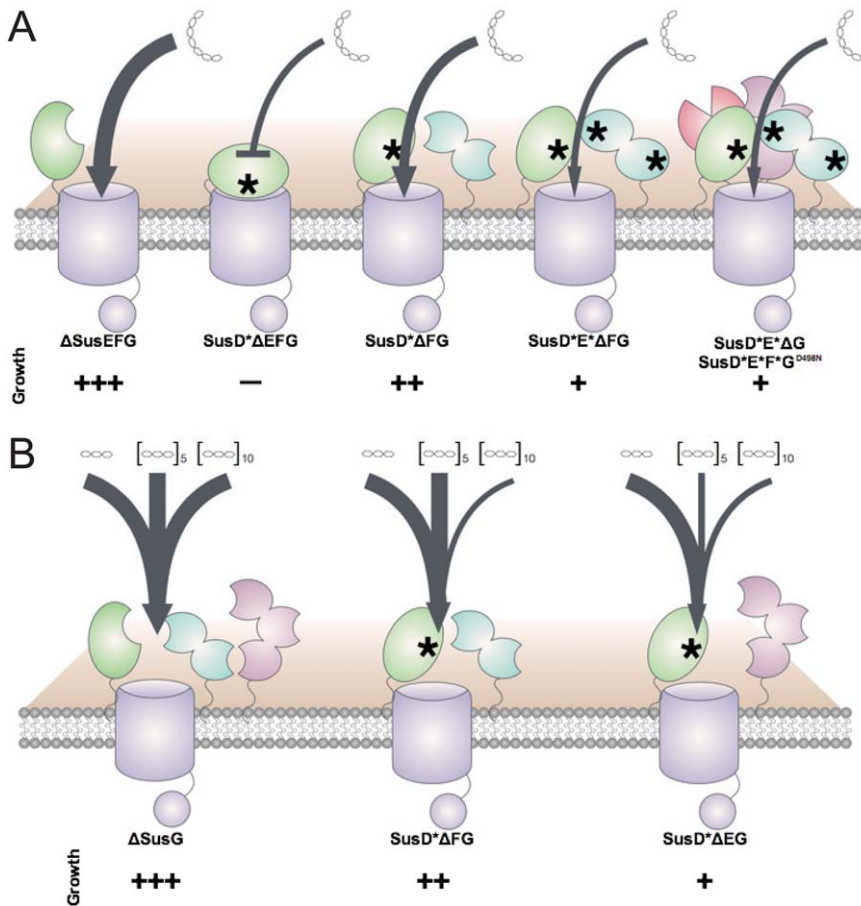


Fig. 7. A model for maltooligosaccharide uptake facilitated by the SusEF starch-binding proteins. Asterisks indicate a site-directed mutant that no longer binds starch. The Sus proteins are colored: SusC, purple; SusD, green; SusE, blue; SusF, magenta; SusG, pink. A. The relative growth of the cells on maltoheptaose is displayed with more + indicating less lag time and more efficient growth. SusEF are not necessary for *in vitro* growth on maltoheptaose, but the presence of SusE is required in a SusD* background. B. The relative growth of the cells on maltooligosaccharides of various DP is displayed with more + indicating a greater maximum O.D. and better utilization of the glycans within the mixture. The thickness of the arrow indicates the ability of the cells to take maltooligosaccharides of DP3, DP15 and DP30. Cells expressing SusCDEF (Δ SusG) can utilize all sizes of maltooligosaccharides, while cells expressing only SusE or SusF in a SusD* background are impaired for the uptake of large and mid- to-large glycans respectively.

lipoproteins, BT2262 and BT2261. BT2261 and BT2262 are comprised of Ig-like folds, akin to SusE and SusF, and wrap around the back of the CD-like complex; these proteins seem to affect the movement of SusD in molecular dynamics simulations, suggesting they contribute to the open/close mechanism of the transporter. However, the precise role of BT2261 and BT2262 in selection of ligand or bacterial growth has not been elucidated.

Glycan-binding lipoproteins akin to SusE and SusF, sometimes referred to as 'SusE-positioned genes' or surface glycan binding protein-B (SGBP-B), functionally differ from SusD and its homologs. The presence of SusD-like proteins is required in some Sus-like systems like that for the uptake of xyloglucan in *B. ovatus* (Tauzin *et al.*, 2016), but is less important for the uptake of levan and not at all for the uptake of fructooligosaccharides in *B. thetaioaomicron* (Sonnenburg *et al.*, 2010). SusEF-like SGBPs are encoded in PULs throughout the gut Bacteroidetes suggesting that they play a critical role in glycan capture (Martens *et al.*, 2009; Martens *et al.*, 2011). However, the importance and nature of their role may vary depending on the

characteristics of the substrate. In the Sus, SusE appears to have evolved an intriguing role in maltooligosaccharide uptake (Fig. 7A). Our data support that SusC and SusD interact to form a high affinity transporter that facilitates efficient growth on maltoheptaose. SusD*, in the absence of other starch-binding proteins, cannot support growth, possibly by stably interacting with SusC and preventing the introduction of sugar into the transporter. This sort of closed complex absent of substrate is seen in the SusCD-like crystal structure of BT1763/1762 (Glenwright *et al.*, 2017). SusE can uniquely resuscitate growth independent of its starch-binding sites, which we speculate is accomplished by SusE interacting with the core SusCD complex and allowing SusD to open for import. Curiously, the starch-binding sites on SusF and SusG do not enhance growth kinetics in a SusD*E* strain. This observation highlights the idea that starch-binding on the cell surface is not sufficient to assist in transport, and that the interaction of SusE with the SusCD transport complex may give it a privileged proximity near the opening of the pore.

That bacteria would evolve glycan uptake systems that import larger oligosaccharides is logical from an

energetics viewpoint – it saves the energy of active transport when larger oligosaccharides can be imported at the same relative energetic ‘cost’ as smaller ones. Although a different type of import system from the Sus, ATP-binding cassette (ABC) transporters for maltodextrins in Gram-positive bacteria such as *Streptococcus pneumoniae* and *Eubacterium rectale* have been observed to specifically target the uptake of oligosaccharides larger than maltose (Abbott *et al.*, 2010; Cockburn *et al.*, 2015). In these cases, the surface digestion of polysaccharide is coordinated with the specificity of the ABC transport solute-binding protein. For example, in *Streptococcus pneumoniae* the surface enzyme SpuA digests glycogen into a ladder of fragments of up to at least 30 residues in length, and the MalX solute-binding protein aids in the transport of maltooligosaccharides of up to 12 residues, based upon the size of the glycans preferentially depleted from culture supernatants of cells grown on glycogen (Abbott *et al.*, 2010). This is in contrast to *E. coli*, in which the maltose-binding protein MalE can apparently transport glycans up to eight or ten glucose residues, but growth defects are observed on maltooligosaccharides larger than maltoheptaose, due in part to the inefficiency of the uptake of these longer sugars (Wandersman *et al.*, 1979; Ferenci, 1980). Despite differences in mechanism, these maltooligosaccharide ABC transporters and the Sus are similar in that they provide a strategy for the specific uptake of maltooligosaccharides, however the Sus may be unique in its ability to target even longer glycans.

Our data suggest that the collection of Sus proteins at the surface may dictate the length of maltooligosaccharides captured by *B. thetaiotaomicron*. Surprisingly, the Δ SusG strain is capable of importing even the longest range of oligosaccharides (DP25–40), as suggested from the lack of detection of these sugars in the culture supernatant, although they are detected in SusD* Δ EG and SusD* Δ FG cultures. Because these sugars are much larger than the substrates targeted by classically studied TonB-dependent transporters (Noinaj *et al.*, 2010), it seems probable that SusC has been adapted to target larger substrates derived from polysaccharides. Indeed, that SusC-like transporters for other complex glycans such as α -mannan, rhamnogalacturonan-II, chondroitin sulfate and heparin or heparan sulfate can import very large oligosaccharides has been suggested or observed (Raghavan *et al.*, 2014; Cuskin *et al.*, 2015; Cartmell *et al.*, 2017; Ndeh *et al.*, 2017). SusG is an endoamylase that can conceivably generate large oligosaccharides when hydrolyzing starch, yet *in vitro* digests yield glucose and maltose (Koropatkin and Smith, 2010). Perhaps at the cell surface, the product profile of SusG is altered to include longer sugars, or the Sus can also sequester long oligosaccharides generated from

neighboring species. Our work has also shown that maltooligosaccharides of varying length can be imported with different efficiencies, and that starch-binding proteins can in part modulate these differences (Fig. 7B). We show here that SusE and SusF can greatly effect the uptake efficiency of maltooligosaccharides at the cell surface. SusD* Δ EG displays a much lower capacity to efficiently transport mid- and long-range maltooligosaccharides of DP5–16. This forces the SusD* Δ EG strain to grow on smaller sugars that provide a poor return on the energetic investment to actively import those substrates. SusD* Δ FG has a similar but less critical deficiency during uptake as well. That these surface glycan-binding proteins can adapt the cell to access different lengths of the same type of glycan is currently unexplored, but it may provide a mechanism explaining how bacteria can partition into nutrient niches or how they can share nutrients while foraging on the same glycans. The Bacteroidetes acquire large, complex and heterogeneous substrates for carbohydrate catabolism in order to remain competitive in the gut ecosystem. A mechanistic understanding of nutrient acquisition in the gut microbiome is a key prerequisite to intelligently manipulating this ecosystem to our benefit (Gordon, 2012; Hutkins *et al.*, 2015).

Experimental procedures

Bacterial strains and culture conditions

For these experiments and to generate all of the mutant *sus* strains used in these experiments, the *B. thetaiotaomicron* VPI-5482 Δ *tdk* strain was employed to facilitate allelic exchange, as previously described (Koropatkin *et al.*, 2008; Cameron *et al.*, 2012), and is the parent strain for all of the mutations within this work. For clarity we refer to the Δ *tdk* strain as wild-type, as this parent strain retains a wild-type *sus* locus. Mutations were generated using the counterselectable allelic exchange vector pExchange-*tdk* as previously described (Koropatkin *et al.*, 2008). The primers used in this study were synthesized by IDT DNA Technologies and are described in Table S3 of the Supporting Information. The *sus* alleles for all Sus* mutants are included in Table 1 and were validated in our previous studies, as referenced. A table of strains used in this study is provided in Supporting Information Table S1. SusE-F chimeric constructs were designed based upon the known structures of these proteins.

Bacteroides thetaiotaomicron was cultured in a 37°C Coy anaerobic chamber (5% H₂/10% CO₂/85% N₂) from freezer stocks into tryptone-yeast extract-glucose (TYG) medium (Holdeman *et al.*, 1977) and grown for 24 h, to an O.D. ~1.0. The following day cells were back-diluted 1:100 into Bacteroides minimal media (MM) including 5 mg ml⁻¹ glucose or maltose (Sigma) as noted and grown overnight (16 h). For kinetic growth experiments in a plate reader, MM-glucose or MM-maltose grown cells were back-diluted

1:200 into MM with the experimental carbohydrate, and in parallel to MM with glucose. Thus both glucose controls and experimental starch and oligosaccharide grown cultures were started at the same initial O.D.₆₀₀ of 0.1 in the plate reader (or 0.02 in a 1 cm path length spectrophotometer at O.D.₆₀₀). All glucose controls for each set of growth experiments are displayed in Supporting Information Fig. S1. The substrates used for comparison to parallel glucose-grown cultures included: 2.5 mg ml⁻¹ (2.17 mM) maltoheptaose (Carbosynth), 5 mg ml⁻¹ maize amylopectin (Sigma) or 5 mg ml⁻¹ DP10–40 (Elicityl). Kinetic growth experiments were performed at 37°C in 96 well plates and O.D.₆₀₀ were recorded every 10–30 min. All plate reader growth experiments were performed in 3–10 replicates and the averages are reported in each figure here. However, all biological experiments were repeated at least twice to verify consistent growth phenotypes from day to day. Manual growth curves were performed in 16 mm glass culture tubes and O.D.₆₀₀ measurements were taken from the same tubes by a Genesys20 spectrophotometer. The spectrophotometer was blanked with media plus maltoheptaose including those curves for the starch media, which has a background absorbance of 0.2. *B. thetaiotaomicron* was cultured in culture tubes as previously specified except cultures were started from 1:800 back-diluted overnight grown cells in MM plus glucose, or maltose for the starch-grown cultures. Specific growth rates were calculated as the $\Delta\text{O.D.}_{600} \Delta\text{time}^{-1} \text{O.D.}_{600}^{-1}$. The change in O.D. was calculated over a 40 min – 1.5 h duration.

Cloning and recombinant protein expression

Chimeric SusE and SusF alleles were PCR amplified from genomic DNA for ligation-independent cloning into pETite N-His vector (Lucigen Madison, WI) according to the manufacturer's instructions. The N-terminal primers introduced a TEV-cleavable site between the mature protein that lacks a signal sequence and the His tag as well as a mutation C21A and C20A of SusE and SusF respectively to produce soluble TEV-cleavable His-tagged proteins. Chimeric SusEF-containing pETite plasmids were transformed into Rosetta (DE3) pLysS cells (EMD Biosciences) and plated on LB agar containing 50 µg ml⁻¹ kanamycin (Kan) and 20 µg ml⁻¹ chloramphenicol (Cm). After 16 h of growth at 37°C, colonies from plates were used to inoculate 1 l of terrific broth plus Kan and Cm for growth at 37°C. Cultures were grown to an O.D.₆₀₀ of ~0.6 before 0.5 mM IPTG was added and cells were grown at room temperature (~20°C) for an additional 20 h. Cells were harvested by centrifugation and cell pellets were flash frozen in liquid N₂ until purification.

Recombinant protein purification

Cell pellets were resuspended in 50 ml of His Buffer (25 mM NaH₂PO₄, 500 mM NaCl, 20 mM imidazole, pH 7.4) and were lysed by sonication. Lysates were centrifuged at 20 000 × g to remove intact cells and the soluble lysate containing His-tagged chimeric SusEF proteins were purified using a 5 ml Hi-Trap metal affinity cartridge (GE Healthcare) charged with NiSO₄ according to the manufacturer's instructions. Cell

lysates were applied to the column in His Buffer and proteins were eluted with an imidazole (20–300 mM) gradient. The His-tag was removed with a 2 h incubation with recombinant TEV (1:100 molar ratio of TEV to protein) at room temperature, followed by an overnight incubation at 4°C while dialyzing into His buffer with 20 mM imidazole. Affinity purification using a Ni-charged Hi-Trap affinity cartridge was repeated to remove the His-tag, uncut protein and His-tagged TEV, while the cleaved protein was collected as the flow through. The protein was then dialyzed against a storage buffer (20 mM HEPES, 100 mM NaCl, pH 7.0) and concentrated using a Vivaspin 15 (10 000 MWCO) centrifugal concentrator (Viva-products, Inc.).

Isothermal titration calorimetry

ITC measurements were performed on a low volume (300 µl sample cell) TA instruments NanoITC. Maltoheptaose (Sigma) solutions were prepared using the same dialysis buffer as the proteins, and thus protein and titrant were in the same buffer for all experiments. For each experiment 97–120 µM protein was placed in the sample cell. The reference cell was filled with deionized water. After the cell temperature was equilibrated to 25°C, an initial injection of 0.25 µl of maltoheptaose was performed followed by 25 subsequent injections of 2 µl of 7 mM maltoheptaose (Sigma). The sample cell was stirred at 250 rpm and the resulting heat of reaction was measured. Data were analyzed using the NanoAnalyze software package (TA instruments) by fitting to an independent binding model and fixing N to the number of known binding sites in the protein. Each titration was performed in triplicate.

Growth competition experiments and quantitative PCR

SusE/F strains used in this competition experiment were tagged with either pNBU2-tag 11 or 14 (Koropatkin *et al.*, 2008). Three biological replicates of SusE/SusF strains were passaged each day for two weeks using a daily 1:100 back-dilution into MM containing 5 mg ml⁻¹ glucose or 5 mg ml⁻¹ maize amylopectin supplemented with 0.5 mg ml⁻¹ maltose. Genomic DNA was harvested from cultures on days 0, 1, 2, 3, 4, 6, 8, 10 and 14 using DNeasy Blood & Tissue kit (Qiagen). Genomic DNA quantification was performed with a Mastercycler® ep realplex (Eppendorf), using KAPA SYBR® FAST qPCR Master Mix and 100 nM SusE and SusF primers, for 40 cycles of 95°C for 3 s, 55°C for 8 s, 72°C for 20 s, followed by a melting step to determine amplicon purity. Samples were normalized to a DNA standard curve of genomic DNA from each respective strain. Relative abundance was calculated as the percent composition of a strain's DNA relative to the total DNA in the sample. Primers used for qPCR are listed in Supporting Information Table S3.

Western blotting

Bacteroides thetaiotaomicron strains were grown in MM containing 5 mg ml⁻¹ maltose and were harvested at

O.D.₆₀₀ = 0.6. Cells were lysed in SDS sample buffer and 15 µg of total protein was loaded into an SDS-PAGE. SusF was detected in *B. thetaiotaomicron* whole cell lysates by western blot using custom rabbit polyclonal primary antibodies and horseradish peroxidase conjugated goat anti-Rabbit IgG secondary antibody (Sigma) (Cameron *et al.*, 2012).

Immunofluorescence

Bacteroides thetaiotaomicron strains were grown in 5 ml minimal *Bacteroides* medium supplemented with 5 mg ml⁻¹ maltose to an O.D.₆₀₀ of 0.6 and then harvested via centrifugation (7000 × *g* for 3 min) and washed twice with phosphate-buffered saline (PBS). Cells were resuspended in 0.25 ml PBS, and 0.75 ml of 6% formalin in PBS was added. Cells were incubated with rocking at 20°C for 1.5 h and then washed twice with PBS. Cells were resuspended in 0.5–1 ml blocking solution (2% goat serum, 0.02% NaN₃ in PBS) and incubated for 16 h at 4°C. Cells were centrifuged and resuspended in 0.5 ml of a 1:100 dilution of custom rabbit anti-SusE or anti-SusF antibody sera in blocking solution and incubated by rocking for 2 h at 20°C. Cells were washed with PBS and then resuspended in 0.4 ml of a 1:500 dilution of Alexa Fluor 488 goat anti-rabbit IgG (Life Technologies) in blocking solution and incubated with rocking for 1 h at 20°C. Cells were washed three times with an excess of PBS and then resuspended in 20 µl of PBS plus 1 µl of ProLong Gold antifade (Life Technologies). Cells were spotted on 0.8% agarose pads and imaged using an Olympus IX70 inverted confocal microscope. Images were processed with Metamorph Software.

Thin layer chromatography

Cell-free culture supernatant was collected from stationary phase ΔSusG cultures grown in minimal media containing 5 mg ml⁻¹ maltose. Supernatant was added to minimal media containing 5 mg ml⁻¹ DP10–40 to make up 5% of the reaction volume. Reactions were incubated at 37°C for 1 hour and then flash frozen. These reactions were spotted onto TLC Silica gel 60 F254 20 × 20 cm glass plates (Millipore) and separated with the solvent acetonitrile:ethyl acetate:isopropanol:water (40:10:25:25) until the solvent front was within 1 cm of the top of the plate. The sugars were then stained with 0.3% (w/v) N-(1-naphthyl)ethylenediamine, 5% (v/v) sulfuric acid in methanol and heated until spots developed.

HPAEC-PAD maltooligosaccharide analysis

Samples were processed by the GlycoAnalytics Core at the University of California San Diego. Crude supernatant samples were passed over a PGC cartridge (poly-graphitized charcoal) HyperSep™ Hypercarb™ SPE Cartridges (Thermo Scientific), washed with 5 ml water and bound oligosaccharides were eluted with 30% Acetonitrile solution containing 0.1% TFA. This purification results in the loss of glucose and maltose. Eluted oligosaccharides were dried,

resuspended in water, and injected on HPAEC-PAD. Oligosaccharide profiling was performed using BioLC CarboPac PA100 column (4 × 250 mm) with PA100 (4 × 50 mm) guard column at a flow rate 1 ml min⁻¹. Pulsed amperometric detection with a gold electrode and standard quad waveform was used for carbohydrate analysis. The elution gradient was as follows: 0.0–20.0 min isocratic flow with 19 mM sodium hydroxide containing 7 mM sodium acetate, 20–70 min linear gradient of 0–400 mM sodium acetate. Maltrin-100 and Maltrin-200 were used as standards to compare the elution time for each oligosaccharide to verify the degree of polymerization. The area under each peak was calculated using Chromeleon™ 6.8 Chromatography Data System software and the DP values were assigned based on the retention time (min). Relative abundance is calculated as the percent composition of an oligosaccharide's peak area relative to the total area of all peaks in the sample.

Acknowledgements

We thank the members of the Koropatkin and Martens labs at the University of Michigan for their support and advice during the design and execution of these studies. Funding for this research was provided by the National Institutes of Health (NIH R01 GM118475 to NMK). M.H.F. was partially supported by a predoctoral fellowship from the Cellular Biotechnology Training Program (T32GM008353).

Author contributions

M.H.F. and N.M.K. designed the study, analyzed the data and wrote the manuscript. M.H.F. performed all of the experiments in this study. E.C.M. provided several of the mutants used in this study, as well as advice and guidance throughout the study design, data analysis and drafting of the manuscript.

References

- Abbott, D.W., Higgins, M.A., Hyrnuik, S., Pluvinaige, B., Lammerts van Bueren, A., and Boraston, A.B. (2010) The molecular basis of glycogen breakdown and transport in *Streptococcus pneumoniae*. *Mol Microbiol* **77**: 183–199.
- Cameron, E.A., Kwiatkowski, K.J., Lee, B.H., Hamaker, B.R., Koropatkin, N.M., and Martens, E.C. (2014) Multifunctional nutrient-binding proteins adapt human symbiotic bacteria for glycan competition in the gut by separately promoting enhanced sensing and catalysis. *mBio* **5**: e01441-14–e01414.
- Cameron, E.A., Maynard, M.A., Smith, C.J., Smith, T.J., Koropatkin, N.M., and Martens, E.C. (2012) Multidomain carbohydrate-binding proteins Involved in *Bacteroides thetaiotaomicron* Starch Metabolism. *J Biol Chem* **287**: 34614–34625.

- Cartmell, A., Lowe, E.C., Basle, A., Firbank, S.J., Ndeh, D.A., Murray, H., Terrapon, N., Lombard, V., Henrissat, B., Turnbull, J.E., Czjzek, M., Gilbert, H.J., and Bolam, D.N. (2017) How members of the human gut microbiota overcome the sulfation problem posed by glycosaminoglycans. *Proc Natl Acad Sci U S A* **114**: 7037–7042.
- Cho, K.H., and Salyers, A.A. (2001) Biochemical analysis of interactions between outer membrane proteins that contribute to starch utilization by *Bacteroides thetaiotaomicron*. *J Bacteriol* **183**: 7224–7230.
- Cockburn, D., and Koropatkin, N.M. (2016) Polysaccharide degradation by the intestinal microbiota and its influence on human health and disease. *J Mol Biol* **428**: 3230–3252.
- Cockburn, D.W., Orlovsky, N.I., Foley, M.H., Kwiatkowski, K.J., Bahr, C.M., Maynard, M., *et al.* (2015) Molecular details of a starch utilization pathway in the human gut symbiont *Eubacterium rectale*. *Mol Microbiol* **95**: 209–230.
- Cuskin, F., Lowe, E.C., Temple, M.J., Zhu, Y., Cameron, E.A., Pudlo, N.A., *et al.* (2015) Human gut Bacteroidetes can utilize yeast mannan through a selfish mechanism. *Nature* **517**: 165–169.
- D'Elia, J.N., and Salyers, A.A. (1996a) Contribution of a neopullulanase, a pullulanase, and an alpha-glucosidase to growth of *Bacteroides thetaiotaomicron* on starch. *J Bacteriol* **178**: 7173–7179.
- D'Elia, J.N., and Salyers, A.A. (1996b) Effect of regulatory protein levels on utilization of starch by *Bacteroides thetaiotaomicron*. *J Bacteriol* **178**: 7180–7186.
- Ding, T., and Schloss, P.D. (2014) Dynamics and associations of microbial community types across the human body. *Nature* **509**: 357–360.
- Elhenawy, W., Debelyy, M.O., and Feldman, M.F. (2014) Preferential packing of acidic glycosidases and proteases into *Bacteroides* outer membrane vesicles. *mBio* **5**: e00909-14–e00914.
- Ferenci, T. (1980) The recognition of maltodextrins by *Escherichia coli*. *Eur J Biochem* **108**: 631–636.
- Flint, H.J., Bayer, E.A., Rincon, M.T., Lamed, R., and White, B.A. (2008) Polysaccharide utilization by gut bacteria: potential for new insights from genomic analysis. *Nat Rev Microbiol* **6**: 121–131.
- Flint, H.J., Duncan, S.H., and Louis, P. (2017) The impact of nutrition on intestinal bacterial communities. *Curr Opin Microbiol* **38**: 59–65.
- Glenwright, A.J., Pothula, K.R., Bhamidimarri, S.P., Chorev, D.S., Basle, A., Firbank, S.J., *et al.* (2017) Structural basis for nutrient acquisition by dominant members of the human gut microbiota. *Nature* **541**: 407–411.
- Gloster, T.M., Turkenburg, J.P., Potts, J.R., Henrissat, B., and Davies, G.J. (2008) Divergence of catalytic mechanism within a glycosidase family provides insight into evolution of carbohydrate metabolism by human gut flora. *Chem Biol* **15**: 1058–1067.
- Gordon, J.I. (2012) Honor thy gut symbionts redux. *Science* **336**: 1251–1253.
- Grondin, J.M., Tamura, K., Dejean, G., Abbott, D.W., and Brumer, H. (2017) Polysaccharide utilization loci: fueling microbial communities. *J Bacteriol* **199**: e00860-16.
- Holdeman, L.V., E.D., Cato, W.E.C. and Moore, (1977) *Anaerobe Laboratory Manual*. Virginia Polytechnic Institute and State University Anaerobe Laboratory, Blacksburg, VA.
- Hutkins, R.W., Krumbek, J.A., Bindels, L.B., Cani, P.D., Fahey, G., Jr., Goh, Y.J., *et al.* (2015) Prebiotics: why definitions matter. *Curr Opin Biotechnol* **37**: 1–7.
- Karunatilaka, K.S., Cameron, E.A., Martens, E.C., Koropatkin, N.M., and Biteen, J.S. (2014) Superresolution imaging captures carbohydrate utilization dynamics in human gut symbionts. *mBio* **5**: e02172-14.
- Koropatkin, N.M., Martens, E.C., Gordon, J.I., and Smith, T.J. (2008) Starch catabolism by a prominent human gut symbiont is directed by the recognition of amylose helices. *Structure* **16**: 1105–1115.
- Koropatkin, N.M., and Smith, T.J. (2010) SusG: A unique cell-membrane-associated alpha-amylase from a prominent human gut symbiont targets complex starch molecules. *Structure* **18**: 200–215.
- Larsbrink, J., Rogers, T.E., Hemsworth, G.R., McKee, L.S., Tausin, A.S., Spadiut, O., *et al.* (2014) A discrete genetic locus confers xyloglucan metabolism in select human gut Bacteroidetes. *Nature* **506**: 498–502.
- Larsbrink, J., Zhu, Y., Kharade, S.S., Kwiatkowski, K.J., Eijssink, V.G., Koropatkin, N.M., *et al.* (2016) A polysaccharide utilization locus from *Flavobacterium johnsoniae* enables conversion of recalcitrant chitin. *Biotechnol Biofuels* **9**: 260.
- Martens, E.C., Koropatkin, N.M., Smith, T.J., and Gordon, J.I. (2009) Complex glycan catabolism by the human gut microbiota: the Bacteroidetes Sus-like paradigm. *J Biol Chem* **284**: 24673–24677.
- Martens, E.C., Lowe, E.C., Chiang, H., Pudlo, N.A., Wu, M., McNulty, N.P., *et al.* (2011) Recognition and degradation of plant cell wall polysaccharides by two human gut symbionts. *PLoS Biol* **9**: e1001221.
- Ndeh, D., Rogowski, A., Cartmell, A., Luis, A.S., Basle, A., Gray, J., *et al.* (2017) Complex pectin metabolism by gut bacteria reveals novel catalytic functions. *Nature* **544**: 65–70.
- Noinaj, N., Guillier, M., Barnard, T.J., and Buchanan, S.K. (2010) TonB-dependent transporters: regulation, structure, and function. *Ann Rev Microbiol* **64**: 43–60.
- Raghavan, V., Lowe, E.C., Townsend, G.E., 2nd, Bolam, D.N., and Groisman, E.A. (2014) Tuning transcription of nutrient utilization genes to catabolic rate promotes growth in a gut bacterium. *Mol Microbiol* **93**: 1010–1025.
- Rakoff-Nahoum, S., Coyne, M.J., and Comstock, L.E. (2014) An ecological network of polysaccharide utilization among human intestinal symbionts. *Curr Biol* **24**: 40–49.
- Reeves, A.R., D'Elia, J.N., Frias, J., and Salyers, A.A. (1996) A *Bacteroides thetaiotaomicron* outer membrane protein that is essential for utilization of maltooligosaccharides and starch. *J Bacteriol* **178**: 823–830.
- Reeves, A.R., Wang, G.R., and Salyers, A.A. (1997) Characterization of four outer membrane proteins that play a role in utilization of starch by *Bacteroides thetaiotaomicron*. *J Bacteriol* **179**: 643–649.
- Renzi, F., Manfredi, P., Mally, M., Moes, S., Jenö, P., and Cornelis, G.R. (2011) The N-glycan glycoprotein deglycosylation complex (Gpd) from *Capnocytophaga canimorsus* deglycosylates human IgG. *PLoS Path* **7**: e1002118.
- Rogowski, A., Briggs, J.A., Mortimer, J., Tryfona, C., Terrapon, T.N., Lowe, E., *et al.* (2015) Glycan complexity dictates microbial resource allocation in the large intestine. *Nat Commun* **6**: 7481.

- Round, J.L., and Mazmanian, S.K. (2009) The gut microbiota shapes intestinal immune responses during health and disease. *Nat Rev Immunol* **9**: 600–323.
- Shipman, J.A., Cho, K.H., Siegel, H.A., and Salyers, A.A. (1999) Physiological characterization of SusG, an outer membrane protein essential for starch utilization by *Bacteroides thetaiotaomicron*. *J Bacteriol* **181**: 7206–7211.
- Smith, K.A., and Salyers, A.A. (1991) Characterization of a neopullulanase and an alpha-glucosidase from *Bacteroides thetaiotaomicron* 95-1. *J Bacteriol* **173**: 2962–2968.
- Sonnenburg, E.D., Zheng, H., Joglekar, P., Higginbottom, S.K., Firbank, S.J., Bolam, D.N., and Sonnenburg, J.L. (2010) Specificity of polysaccharide use in intestinal bacteroides species determines diet-induced microbiota alterations. *Cell* **141**: 1241–1252.
- Stappenbeck, T.S., Hooper, L.V., and Gordon, J.I. (2002) Developmental regulation of intestinal angiogenesis by indigenous microbes via Paneth cells. *Proc Natl Acad Sci U S A* **99**: 15451–15455.
- Tamura, K., Hemsworth, G.R., Dejean, G., Rogers, T.E., Pudlo, N.A., Urs, K., *et al.* (2017) Molecular mechanism by which prominent human gut Bacteroidetes utilize mixed-linkage beta-glucans, major health-promoting cereal polysaccharides. *Cell Rep* **21**: 417–430.
- Tancula, E., Feldhaus, M.J., Bedzyk, L.A., and Salyers, A.A. (1992) Location and characterization of genes involved in binding of starch to the surface of *Bacteroides thetaiotaomicron*. *J Bacteriol* **174**: 5609–5616.
- Tauzin, A.S., Kwiatkowski, K.J., Orlovsky, N.I., Smith, C.J., Creagh, A.L., Haynes, C.A., *et al.* (2016) Molecular dissection of xyloglucan recognition in a prominent human gut symbiont. *mBio* **7**: e02134-15–e02115.
- Terrapon, N., Lombard, V., Gilbert, H.J., and Henrissat, B. (2015) Automatic prediction of polysaccharide utilization loci in Bacteroidetes species. *Bioinformatics* **31**: 647–655.
- Tuson, H.H., Foley, M.H., Koropatkin, N.M., and Biteen, J.S. (2018) The starch utilization system assembles around stationary starch-binding proteins. *Biophys J pii: S0006-3495*: 35095-6.
- Wandersman, C., Schwartz, M., and Ferenci, T. (1979) *Escherichia coli* mutants impaired in maltodextrin transport. *J Bacteriol* **140**: 1–13.
- Wardwell, L.H., Huttenhower, C., and Garrett, W.S. (2011) Current concepts of the intestinal microbiota and the pathogenesis of infection. *Curr Infect Dis Rep* **13**: 28–34.
- Ze, X., Duncan, S.H., Louis, P., and Flint, H.J. (2012) *Ruminococcus bromii* is a keystone species for the degradation of resistant starch in the human colon. *ISME J* **6**: 1535–1543.

Supporting information

Additional supporting information may be found in the online version of this article at the publisher's web-site.